Sequence-Based Hazard Maps for the United Kingdom

Mabel Orlacchio[1], Pasquale Cito[1], Barbara Polidoro[2], Manuela Villani[3], and Iunio Iervolino[*1]

ABSTRACT

The current practice of probabilistic seismic hazard analysis (PSHA) does not take into account that earthquakes actually occur in time–space clusters. The input for PSHA is based on declustered seismic catalogs, used to characterize only the mainshocks, that is, the largest magnitude events within each cluster. However, the so-called sequence-based PSHA (SPSHA; Iervolino *et al.*, 2014) allows us including the effect of aftershocks in hazard analysis, that is, the events following the mainshock, still conveniently resourcing from declustered catalogs. In the United Kingdom (UK), the seismic source model developed for the national seismic hazard assessment has been recently updated by the British Geological Survey (BGS, 2020). In this study, the source model developed by the BGS (one directly derived from it, in fact) is used to implement SPSHA in the UK. The calibration of the model for the occurrence of aftershocks, that is, the modified Omori's law, is fitted on a few sequences and under some simplifying assumptions. The results, represented by hazard maps for selected spectral ordinates and exceedance return periods of interest for structural engineering, are compared to the PSHA counterparts to discuss the increase in the design seismic actions when the effects of aftershocks are considered. The maps show that, based on the modeling of aftershock sequences considered in the study, in the UK this increase can be up to 14%, at least for the spectral ordinates and exceedance return periods herein investigated. The discussed maps are provided as supplemental material to this article.

KEY POINTS

- New seismic hazard maps for the UK were developed.
- The seismic hazard assessment includes the effect of aftershocks.
- It was found that the increments with respect to classical PSHA are lower than 20%.

Supplemental Material

INTRODUCTION

In the United Kingdom (UK), design seismic actions for structural design are based on probabilistic seismic hazard analysis (PSHA; McGuire, 2004). For a given ground motion intensity measure (*IM*), PSHA allows us to compute the rate of seismic events causing exceedance of a selected threshold at the site of interest. In the classical PSHA, the rate of exceedance is time invariant and defines the homogenous Poisson process (HPP) describing the occurrence of earthquakes causing exceedance of the ground motion *IM* threshold over time (Cornell, 1968).

Although earthquakes typically occur in spatiotemporal clusters, classical PSHA complies with the HPP assumption of earthquakes occurrence considering only the largest magnitude event within each cluster, conventionally recognized as the mainshock, whereas (the effects of) the other events in the cluster are neglected. To achieve this, seismicity parameters for the definition of the input models used for PSHA are derived from a catalog in which foreshocks and aftershocks, that is, the earthquakes preceding and following the mainshock, respectively, are preliminarily removed using declustering techniques (e.g., Gardner and Knopoff, 1974).

For short-term risk management purposes, Yeo and Cornell (2009) developed aftershock PSHA (APSHA), which provides the probability that aftershocks in a given time interval cause exceedance of a ground motion *IM* value at the site of interest. In the framework of APSHA, occurrence of aftershocks in time is characterized by means of a nonhomogeneous Poisson process (NHPP), conditional to the occurrence of a mainshock of given magnitude and location, and for which the rate is modeled according to the modified Omori law (Utsu, 1961), although, in

1. Dipartimento di Strutture per l'Ingegneria e l'Architettura, Università degli Studi di Napoli Federico II, Naples, Italy, https://orcid.org/0000-0001-6603-8106 (PC); https://orcid.org/0000-0002-4076-2718 (II); 2. Arup, Milan, Italy; 3. Arup, London, United Kingdom

*Corresponding author: iunio.iervolino@unina.it

Cite this article as Orlacchio, M., P. Cito, B. Polidoro, M. Villani, and I. Iervolino (2022). Sequence-Based Hazard Maps for the United Kingdom, *Bull. Seismol. Soc. Am.* **112**, 2124–2140, doi: 10.1785/0120210189

principle, other models describing aftershock occurrence can be embedded in APHSA in lieu of the modified Omori law.

Iervolino *et al.* (2014) showed that it is possible to include the effects of aftershocks in long-term hazard assessment, avoiding the violation of the HPP hypothesis and possible catalog incompleteness with respect to aftershocks, using the so-called sequence-based PSHA (i.e., SPSHA). Acknowledging that mainshock–aftershocks sequences occur at the same rate as the mainshocks, SPSHA combines PSHA and APSHA resulting in a relatively easy-to-implement hazard integral, which allows us to compute the rate of mainshock–aftershock sequences causing exceedance of a given *IM* threshold at the site. Because SPSHA models the occurrence of aftershocks by means of the modified Omori law, it neglects foreshocks that, although can also possibly contribute to hazard, are generally considered of minor relevance to structural engineering with respect to aftershocks (Yeo and Cornell, 2009).

Before proceeding any further, it is to note that there are other approaches that allow to account for earthquake clusters in seismic hazard analysis (e.g., Marzocchi and Taroni, 2014; Zhang *et al.*, 2018, 2021; Papadopoulos *et al.*, 2021). One of these approaches, which is often assumed as a benchmark by seismologists, is the one referred to as epidemic-type aftershock sequences (ETAS; Ogata, 1988). However, Wang *et al.* (2021), considering a point source model, as well as Sipcic *et al.* (2022), recently discussed that the differences on hazard results between SPSHA- and ETAS-based seismic hazard analysis are of limited relevance, if any, for earthquake engineering purposes.

Recently, the British Geological Survey (BGS, 2020) has developed new PSHA-based hazard maps for the UK. The study presented herein, similar to what was done in Iervolino *et al.* (2018) and Chioccarelli *et al.* (2021) for Italy, aims to investigate the implications, on the definition of design seismic actions in the UK, stemming from including seismic sequences in hazard analysis. To do so, the SPSHA procedure is developed at the national scale, using a simplified yet validated version of the BGS source model, in which the validation consists of comparing the PSHA results against the official BGS counterpart. The parameters of the modified Omori law, required by SPSHA, are calibrated based on a few sequences (because of a general paucity of aftershock data in the UK) from a catalog developed for the UK (Villani *et al.*, 2020).

The SPSHA results for the entire country are presented by hazard maps in terms of (5% damped) spectral (pseudo) accelerations (*Sa*) at three vibration periods (T), as the *IMs*, and for four exceedance return periods (T_r) of structural design interest. Subsequently, SPSHA results are compared to those from PSHA, implemented using the simplified hazard model, to discuss the effects of aftershocks on design seismic actions in the UK.

The article is structured such that the essentials of SPSHA are recalled first. Then, the source model is introduced followed by the calibration of the modified Omori law for the UK. After presenting the hazard maps, the hazard increases due to aftershocks countrywide are discussed by comparing SPSHA results to the PSHA counterpart. Moreover, considering three sites in the UK exposed to comparatively low, mid, and high seismic hazard, the aftershock effects are explored with reference to a wide range of spectral ordinates and return periods, using uniform hazard spectra (UHS). A simple sensitivity analysis of results to the parameters of the modified Omori law precedes some final remarks that close the study.

CLASSICAL AND SEQUENCE-BASED PSHA

Classical PSHA provides the average number of mainshocks per unit time (often in one year) causing exceedance of a *IM* threshold (*im*) at the site of interest, that is, the exceedance rate, $\lambda_{im,E}$. This rate is time invariant and defines the HPP regulating the occurrence of earthquakes causing exceedance of *im* over time. Classically, $\lambda_{im,E}$ is computed using equation (1), that is, the hazard integral, which is herein written considering a single seismic source zone affecting the site (e.g., Kramer, 1996):

$$\lambda_{im,E} = \nu_E \cdot \int_{r_{E,\min}}^{r_{E,\max}} \int_{m_{E,\min}}^{m_{E,\max}} P[IM_E > im | M_E = m, R_E = r, \underline{\theta}] \cdot f_{M_E,R_E}(m,r) \cdot dm \cdot dr. \quad (1)$$

The subscript E is added to distinguish the rate $\lambda_{im,E}$ from the rate evaluated using SPSHA, to follow. In the equation, ν_E is the rate of mainshocks with magnitude equal to or larger than the minimum ($m_{E,\min}$) deemed possible for the source, and it is calibrated based on a declustered catalog. The $f_{M_E,R_E}(m,r)$ term is the joint probability density function (PDF) of the mainshock magnitude (M_E) and source-to-site distance (R_E). Assuming that M_E and R_E are stochastically independent random variables, it is $f_{M_E,R_E}(m,r) = f_{M_E}(m) \cdot f_{R_E}(r)$, in which $f_{M_E}(m)$ and $f_{R_E}(r)$ are the marginal distributions of magnitude and distance of mainshocks, respectively. The distribution of magnitude is defined between $m_{E,\min}$ and the maximum magnitude considered for the source, $m_{E,\max}$, and it is generally described by a truncated exponential distribution derived by the Gutenberg–Richter (GR) relationship (Gutenberg and Richter, 1944). The distribution of the distance, which is defined between $r_{E,\min}$ and $r_{E,\max}$, generally only depends on the geometry of the source and the position of the site with respect to the source itself. The term $P[IM_E > im | M_E = m, R_E = r, \underline{\theta}]$, provided by a ground-motion prediction equation (GMPE), represents the conditional probability that *im* is exceeded due to a mainshock with magnitude equal to m and source-to-site distance equal to r. This probability also depends on $\underline{\theta}$, which allows us to account for additional parameters such as local soil site conditions, rupture mechanism of the source and/or others. Considering multiple sources only entails the summation of $\lambda_{im,E}$ referring to each source.

SPSHA allows us to account for the effect of aftershocks (i.e., neglecting foreshocks) in the hazard assessment, using the same input as in the case of PSHA, that is, the rate of mainshocks from a declustered catalog, and modeling the occurrence of aftershocks using a NHPP, conditional to the mainshock magnitude and location. In these hypotheses, the main result of SPSHA is the average number of seismic sequences that cause at least one exceedance of *im* at the site in the unit time. This rate, herein referred to as λ_{im}, defines the HPP process regulating the occurrence of mainshocks, and following aftershocks, that cause exceedance of *im* over time, and it is computed via equation (2):

$$\lambda_{im} = \nu_E \cdot \left\{ 1 - \int_{r_{E,\min}}^{r_{E,\max}} \int_{m_{E,\min}}^{m_{E,\max}} P[IM_E \le im | M_E = m, R_E = r, \underline{\theta}] \times e^{-E[N_{A|m}(0,\Delta T_A)] \cdot \int_{r_{A,\min}}^{r_{A,\max}} \int_{m_{A,\min}}^{m} P[IM_A > im | M_A = m_A, R_A = r_A, \underline{\theta}] \cdot f_{M_A,R_A|M_E,R_E}(m_A, r_A | m, r) \cdot dm_A \cdot dr_A} \cdot f_{M_E,R_E}(m, r) \cdot dm \cdot dr \right\}. \quad (2)$$

In the equation, the (A) subscript denotes terms pertaining to aftershocks. $P[IM_E \le im | M_E = m, R_E = r, \underline{\theta}]$ is equal to $1 - P[IM_E > im | M_E = m, R_E = r, \underline{\theta}]$, whereas the exponential term represents the probability that none of the aftershocks, triggered by the mainshock with magnitude $M_E = m$ and distance $R_E = r$ (strictly speaking, it should be location rather than distance), causes exceedance of *im* between $t = 0$ (i.e., the occurrence time of the mainshock) and the duration of the sequence, ΔT_A. $P[IM_A > im | M_A = m_A, R_A = r_A, \underline{\theta}]$, which is provided by the GMPE, is the probability that *im* is exceeded, given an aftershock of magnitude $M_A = m_A$ and source-to-site distance $R_A = r_A$. The term $f_{M_A,R_A|M_E,R_E}$ is the joint PDF of magnitude and distance of aftershocks, which is conditional on the features of the mainshock (i.e., magnitude and location) occurring on the source. Assuming that M_A and R_A are conditionally independent random variables, it is $f_{M_A,R_A|M_E,R_E} = f_{M_A|M_E} \cdot f_{R_A|M_E,R_E}$, in which $f_{M_A|M_E}$ is the conditional distribution of aftershocks magnitude (i.e., following a GR model), and $f_{R_A|M_E,R_E}$ is the conditional distribution of the distance of the site to aftershocks. The magnitude distribution of the aftershocks is bounded by a minimum magnitude, $m_{A,\min}$, and m (i.e., the mainshock magnitude). The location of aftershocks with respect to the site depends on the location and magnitude of the mainshock. The distribution of the aftershocks distance is bounded within $r_{A,\min}$ and $r_{A,\max}$, which are the minimum and maximum values possible for R_A, respectively. $E[N_{A|m}(0, \Delta T_A)]$ is the expected number of aftershocks, with magnitude between $m_{A,\min}$ and m, generated by a mainshock with magnitude $M_E = m$, in ΔT_A, and it is computed according to Yeo and Cornell (2009):

$$E[N_{A|m}(0,\Delta T_A)] = \frac{10^{a+b\cdot(m-m_{A,\min})} - 10^{a}}{p-1} \cdot \left[c^{1-p} - (\Delta T_A + c)^{1-p} \right], \quad (3)$$

where c and p are the parameters of the modified Omori law, which in fact models the temporal decay of the aftershocks' rate, whereas a and b define the GR relationship for aftershocks.

Computing equation (1) and equation (2) for different *im* values in a range of interest provides the hazard curve for PSHA and SPSHA, respectively. Hazard curves for different spectral ordinates, in turn, allow retrieving the UHS, that is, the spectrum whose ordinates (when considered individually) have the same exceedance return period for the site of interest. Hereafter, the PSHA- and SPHA-based UHS ordinates will be indicated as sa_{PSHA} and sa_{SPSHA}, respectively. Obviously, it is $\lambda_{im} \ge \lambda_{im,E}$ for any *im* value; thus given the return period, it is, $sa_{SPSHA} \ge sa_{PSHA}$.

SEISMIC HAZARD MODEL

BGS logic tree

Both PSHA and SPSHA presented in this work were implemented using the source model recently updated by the BGS. The PSHA study of the BGS features a complex logic tree consisting of several branches. In each branch, the source model is based on 22 seismic source zones, the geometry of which and ID are shown in Figure 1 (together with five sites of interest that will be considered later). The source model is defined on the basis of the current understanding of seismicity in the UK, taking also into account the surrounding areas that are considered to have some impact on the seismic hazard of the country, that is, the Viking graben (VIKI), the Normandy (NORM), and the Belgium-Pas de Calais region (PASC). For each zone, the expected magnitude frequency distribution of the earthquakes follows a GR relationship, with a minimum magnitude equal to 3.0. The uncertainties affecting the seismicity parameters of the zones are taken into account using 100 branches of the logic tree, varying in terms of maximum magnitude, b-value and annual rate of mainshocks with (moment) magnitude equal to or larger than 3.0, $\nu_E(M \ge 3.0)$. More specifically, according to the logic tree, four maximum magnitudes (i.e., 6.5, 6.7, 6.9, and 7.1) and 25 couples of the b– values and $\nu_E(M \ge 3.0)$ are identified for each source zone.

Considering the mean of the 25 $\nu_E(M \ge 3.0)$ values, which is also provided by the BGS for each source zone, one can observe that the lowest $\nu_E(M \ge 3.0)$ is 0.0037 events per year for the zone named BALA, whereas the largest rate (1.12 events per year) is for the MMCW zone. It is worth noting that seismicity for two zones, that is, MMCW and MENA, is defined

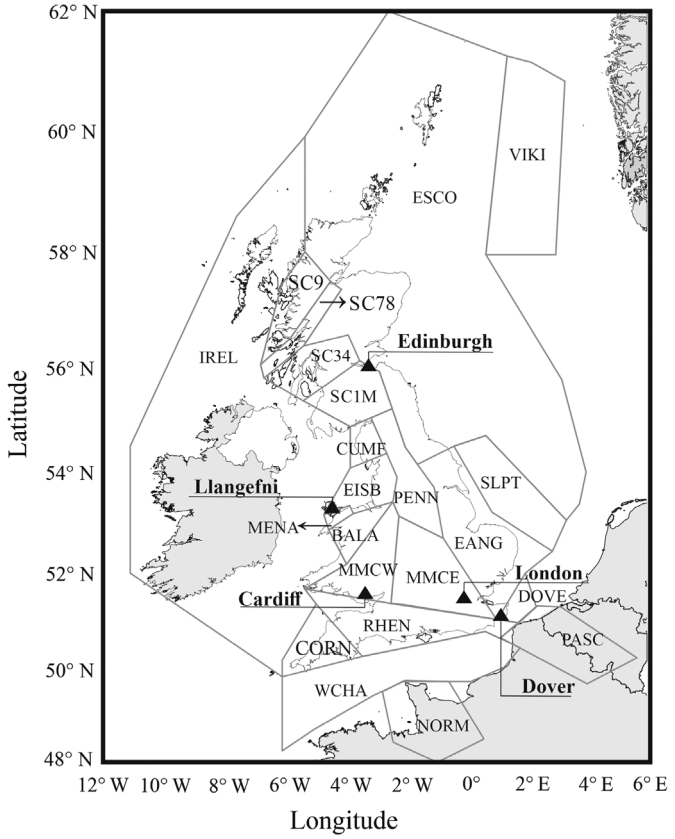

Figure 1. The seismic source model used in this study with zone IDs and location of five sites.

using a bipartite GR magnitude distribution (BGS, 2020). The first GR distribution models the occurrence of mainshocks in the range of magnitude between 3.0 and 4.5, whereas the other applies between 4.5 and $m_{E,\max}$.

Both BALA and MMCW zones are located in the western part of the UK; in the remaining part of the country, the rate of earthquakes with magnitude equal to or larger than 3.0 is between 0.1 and 0.47 events per year.

The logic tree implemented by the BGS also accounts for the uncertainty affecting the hypocentral depth considering four possible values, that is, 5, 10, 15, and 20 km. Strike-slip is the dominant rupture mechanism for all the seismic sources.

The BGS study follows the same multi-GMPE approach used in Tromans *et al.* (2019), which considers five GMPEs: Atkinson and Boore (2006, 2011), Rietbrock *et al.* (2013), Bindi *et al.* (2014), Boore *et al.* (2014), and Cauzzi *et al.* (2015). These populate the logic tree with different weights. Bindi *et al.* (2014) and Boore *et al.* (2014) are given the largest weight, 0.3; Cauzzi *et al.* (2015) is given 0.2, whereas 0.1 is assumed for Atkinson and Boore (2006, 2011) and Rietbrock *et al.* (2013). To account for both the effects of elastic amplification due to shear-wave velocity structure and near-surface attenuation specific for the UK, the host-to-target adjustments (Cotton *et al.*, 2006; Atik *et al.*, 2014) are applied to each of the five GMPEs. The adjustment factors were developed considering rock site conditions and three values of the target spectral decay parameter: 0.016, 0.027, and 0.047 s.

Simplified seismic source and ground-motion models

In this study, the BGS seismic hazard model was adopted for developing both PSHA and SPSHA, yet with some simplifications aimed at avoiding the implementation of the full logic tree. More specifically, for each seismic zone, the GR relationship was defined by considering the weighted mean values (over the 25 values in the BGS study) of $\nu_E(M \geq 3.0)$ and b-values. The maximum magnitude was set equal to 6.5 for all the sources, which corresponds to the value of the branch with the largest weight.

Among the two GMPEs with the highest weight in the BGS work, the one of Bindi *et al.* (2014) was selected and used to compute both $P[IM_E \leq im | M_E = m, R_E = r, \underline{\theta}]$ and $P[IM_A > im | M_A = m_A, R_A = r_A, \underline{\theta}]$ in equation (2). This GMPE adopts the Joyner–Boore distance (R_{JB}; Joyner and Boore, 1981) up to 300 km. In the analyses, assuming a uniform distribution for earthquakes epicenters (both mainshocks and aftershocks), epicentral distance (R_{EPI}) was converted to R_{JB} according to equation (4), which is given by (Montaldo *et al.*, 2005).

$$R_{JB} = 3.5525 + 0.8845 \cdot R_{EPI}. \tag{4}$$

The selected GMPE has a magnitude range of applicability between 4.0 and 7.6; therefore, to avoid extrapolation, earthquakes with magnitude lower than 4.0 were not considered in the hazard assessment (also considering that earthquakes with magnitude lower than 4.0 are typically not of interest to earthquake engineering). Consequently, for each source $\nu_E(M \geq 3.0)$ (i.e., that provided by the BGS) was reduced, according to the GR, to exclude earthquakes with magnitude less than 4.0, which is, therefore, the minimum magnitude considered herein for both PSHA and SPSHA (this is also in agreement with the PSHA analyses carried out by the BGS). Similarly, portions of sources at distances larger than 300 km were not considered in the analyses. The predominant strike-slip style was attributed via terms provided by Bindi *et al.* (2014) for that rupture mechanism. Table 1 summarizes all the source characteristics finally considered.

The PSHA and SPSHA discussed in the following were developed assuming the average shear-wave velocity of the upper 30 m equal to 800 m/s (i.e., rock site conditions) at all the sites. Moreover, the GMPE was corrected to account for the host-to-target adjustment, considering the median value of spectral decay parameter equal to 0.027 s, which is the value corresponding to the branch with the largest weight in the logic tree defined by the BGS. The adjustment factors developed by the BGS for the GMPE of Bindi *et al.* (2014) and used in this study are equal to 1.24, 1.19, and 1.06 for peak

TABLE 1
Mainshocks Seismicity Parameters of Seismic Zones Considered (MENA and MMCW Zones are Reported Twice Because of Their Bipartite Gutenberg–Richter)

Zone	$m_{E,min}$	$m_{E,max}$	*b*-Value	$\nu_E(M \geq 4.0)$ (Events Per Year)
CORN	4.0	6.5	1.03	5.60×10^{-03}
RHEN	4.0	6.5	1.00	5.00×10^{-03}
WCHA	4.0	6.5	0.99	1.33×10^{-02}
DOVE	4.0	6.5	1.00	6.00×10^{-03}
SLPT	4.0	6.5	0.97	1.82×10^{-02}
EANG	4.0	6.5	0.99	1.13×10^{-02}
MMCE	4.0	6.5	0.96	7.68×10^{-03}
PENN	4.0	6.5	0.94	2.64×10^{-02}
MMCW1	4.0	4.5	1.01	1.17×10^{-02}
MMCW2	4.5	6.5	1.02	9.71×10^{-02}
MENA1	4.0	4.5	1.01	6.84×10^{-03}
MENA2	4.5	6.5	1.00	3.16×10^{-02}
EISB	4.0	6.5	0.99	8.19×10^{-03}
CUMF	4.0	6.5	1.02	5.73×10^{-03}
BALA	4.0	6.5	1.00	3.70×10^{-04}
SC1M	4.0	6.5	1.01	1.95×10^{-03}
SC34	4.0	6.5	1.00	1.20×10^{-02}
SC78	4.0	6.5	0.99	1.84×10^{-02}
SC9	4.0	6.5	1.04	1.55×10^{-02}
ESCO	4.0	6.5	1.00	1.50×10^{-02}
IREL	4.0	6.5	1.01	2.93×10^{-03}
VIKI	4.0	6.5	1.01	4.59×10^{-02}
NORM	4.0	6.5	0.86	5.11×10^{-02}
PASC	4.0	6.5	1.00	1.90×10^{-02}

b-value is the parameter defining the Gutenberg–Richter relationship for mainshocks; $m_{E,max}$ is the maximum magnitude of mainshocks; $m_{E,min}$ is the minimum magnitude of mainshocks; and $\nu_E(M \geq 4.0)$ is the rate of mainshocks with (moment) magnitude equal to or larger than four.

ground acceleration (*PGA*), $Sa(T = 0.2\text{ s})$, and $Sa(T = 1.0\text{ s})$, respectively, that is, the *IMs* considered for the hazard maps discussed in the following. The adjustments do not depend on magnitude and source-to-site distance, and apply to the mean of the GMPE, that is, they correspond to a so-called linear effect. Therefore, herein the adjustment factors are applied directly modifying a posteriori the ordinates of the unadjusted UHS of interest, as discussed in Iervolino (2016), which has been shown to be a rigorous procedure in case of GMPEs with linear effects.

Validation

The simplifications to the BGS source model do not affect the results concerning the aftershocks effect on the hazard assessment (to follow), as PSHA and SPSHA are performed using the same input data. However, the results of PSHA conducted via the simplified source model for the sites of Cardiff, Dover, Edinburgh, and London (see Fig. 1 for the location of the sites) are compared to those obtained within the BGS study (Mosca *et al.*, 2022). Figure 2 shows the comparisons in terms of UHS and hazard curves for the four sites. Figure 2a,b describes the UHS computed by the BGS and those developed in this study for the return periods of 475 yr and 2475 yr, respectively. The second row of Figure 2 shows the hazard curves in terms of *PGA* (Fig. 2c) and spectral (pseudo) accelerations corresponding to the vibration period equal to 0.2 s (Fig. 2d) and 1.0 s (Fig. 2e) evaluated for the four sites.

The figure shows that the results obtained using the simplified input model are in a good agreement with those obtained considering the full logic tree, even if some differences can be found. To measure them, the absolute differences between the spectral ordinates obtained in this study and those from the BGS work were quantified for 17 spectral ordinates, in a range of vibration periods between 0 and 3.0 s. For example, considering $T_r = 475$ yr, which is a typical return period in structural design, those differences, on average, are equal to $0.0027g$, $2.23 \times 10^{-04}g$, $0.0012g$, and $0.0011g$ for Cardiff, Dover, Edinburgh, and London, respectively.

Aftershock occurrence model

The parameters $\{a, b, c, p\}$ in equation (3), required for SPSHA, are typically calibrated empirically via data from multiple aftershock sequences for the region of interest; for example, Reasenberg and Jones (1989) for California and Lolli and Gasperini (2003) for Italy. For the UK, to the authors' knowledge, there are no specific studies available. To overcome this issue, two earthquake catalogs were preliminarily investigated. One is that provided by the BGS, which includes 73 mainshock–aftershocks sequences occurring in the whole UK and the surrounding areas. The second one is that of Villani *et al.* (2020), containing 213 earthquakes attributed to 48 mainshock–aftershocks sequences occurring within 300 km from Anglesey, north Wales; see Villani *et al.* (2020) for a map of the events.

The $\{a, c, p\}$ parameters were estimated for each sequence using the maximum likelihood method (e.g., Ogata, 1983; Utsu and Ogata, 1995). However, convergence issues have arisen for the short sequences, that is, those with less than five aftershocks, which are 71 and 44 in the BGS catalog and the Villani *et al.* (2020) catalog, respectively. Moreover, there is no sufficient information about the events in the BGS catalog, and therefore they were neglected. Thus, only the four sequences from the catalog of Villani *et al.* (2020) were considered for calibrating the parameters of the modified Omori law. For the selected sequences, Table 2 shows the ID according to the considered catalog, the event name, the date and time of the mainshock, latitude, and longitude of the epicenter of the mainshock, the mainshock magnitude, the minimum magnitude of aftershocks and the number of aftershocks in each sequence N_{aft}.

For each sequence, the $\{a, c, p\}$ parameters were calibrated by setting the *b*–value equal to one (Helmstetter, 2003). The mean values that are used for the SPSHA are $a = -1.71$, $c = 0.002$, and $p = 0.68$. To qualitatively assess the goodness-of-fit of these parameters, Figure 3 represents the ratio

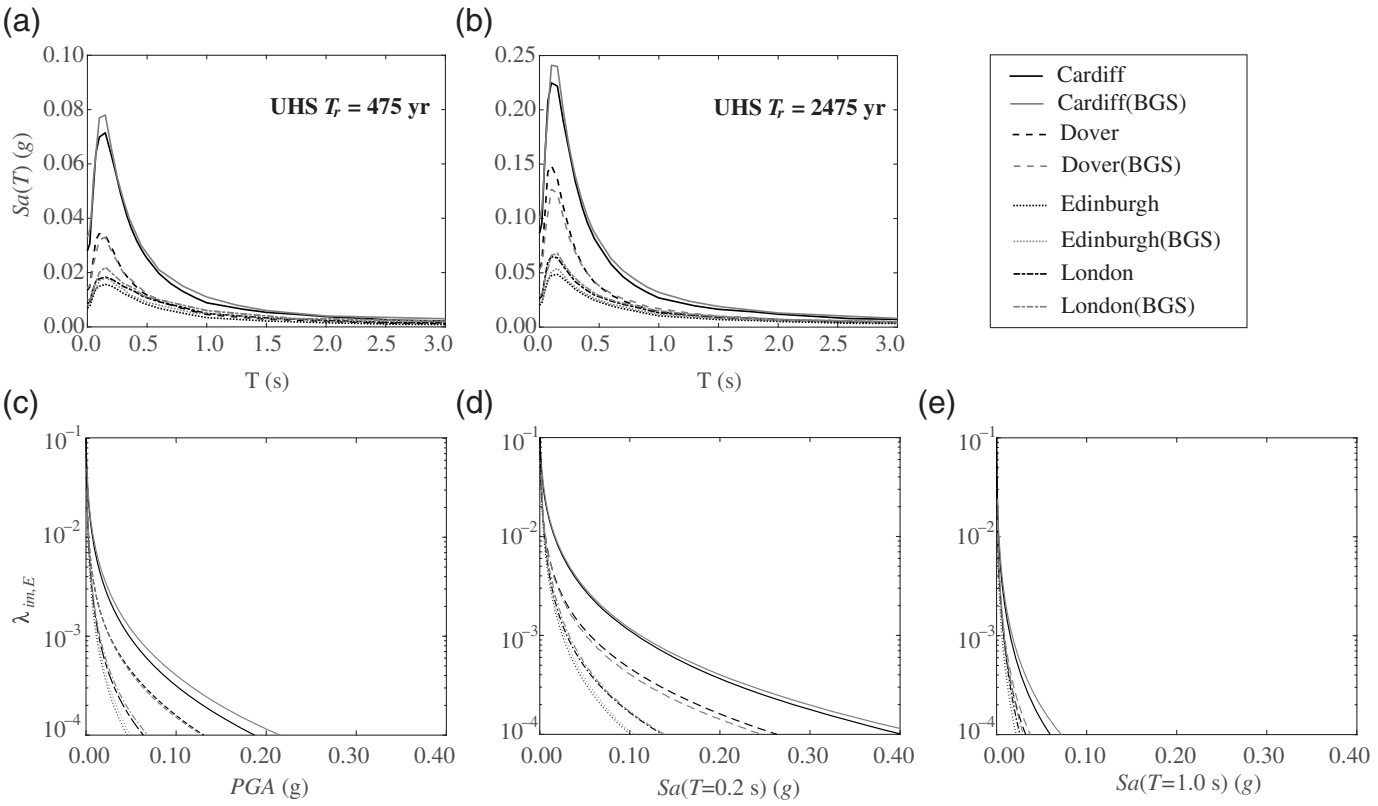

Figure 2. Comparison of the results obtained in the study using probabilistic seismic hazard analysis (PSHA) to the British Geological Survey (BGS) counterparts in terms of uniform hazard spectra (UHS) with (a) $T_r = 475$ yr and (b) $T_r = 2475$ yr, and hazard curves for (c) *PGA*, (d) $Sa(T = 0.2$ s), and (e) $Sa(T = 1.0$ s) for the sites of Cardiff, Dover, Edinburgh, and London.

of the cumulative number of aftershocks within each sequence, $N_A(t)$, as a function of the time t elapsed since the mainshock (expressed in days), to the term $10^{a+b(m-m_{A,\min})}$, that is, the aftershock productivity of each sequence.

It is worth noting that, generally, the uncertainty of $\{a, c, p\}$ may also be quantified (e.g., Ogata, 1978; Kutoyantis, 1982), but the discussed paucity of data would require to adopt approaches such as multimodel inference methods (e.g., Zhang and Shields, 2018); however, this is considered of secondary importance, and it is left out of the scopes of the study.

Moreover, the small dataset of sequences has led to a relatively simple calibration. In other words, the considered aftershock sequences are those assumed to be complete above the minimum aftershock magnitude assumed in SPSHA, which is $m_{A,\min} = 4.0$, that is, the minimum magnitude of the considered GMPE. On the other hand, fitting the Omori parameters using only part of the sequences included in the catalog (i.e., possibly neglecting the low-productivity sequences) may impair the estimation of the average aftershock productivity, as also discussed by Page *et al.* (2016) and Hardebeck *et al.* (2018). However, the implications on the SPSHA results of using different sets of Omori parameters are explored to some extent in the Sensitivity analysis section.

To complete the characterization of the aftershocks in the framework of SPSHA, a model for aftershocks location is needed, which in turn serves to compute $f_{R_A|M_E,R_E}$ in equation (2). Similar to the previous studies (Iervolino *et al.*,

TABLE 2
List of Sequences Detected in the Earthquake Catalog Having a Number of Aftershocks Greater Than Five

Seq. ID	Event Name	Date (yyyy/mm/dd)	Time (hh:mm)	Lat	Long	$M_E = m$	$m_{A,\min}$	N_{aft}
155	Caernarvon	1903/06/19	10:40	53.03°	−4.28°	4.60	2	14
200	Caernarvon	1940/12/12	21:20	53.03°	−4.18°	4.40	2	7
313	Lleyn peninsula	1984/07/19	06:56	52.96°	−4.28°	5.00	2	22
515	Manchester	2002/10/21	11:42	53.48°	−2.20°	2.90	2	51

Lat is the latitude of the epicenter of the mainshock; Long is the longitude of the epicenter of the mainshock; $m_{A,\min}$ is the minimum magnitude of aftershocks; $M_E = m$ is the mainshock magnitude; N_{aft} is the number of aftershocks in each sequence; and Seq. ID is the sequence ID according to the considered catalog.

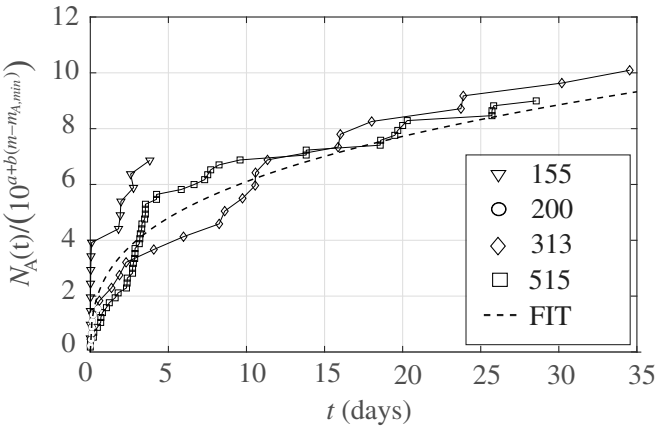

Figure 3. Representation of the four sequences detected for the UK. The smooth curve represents the modified Omori formula obtained using the mean values of the parameters {*a*, *c*, *p*}.

2014, 2018; Chioccarelli *et al.*, 2021), it was assumed that aftershocks may occur with the same probability within a circular area centered on the mainshock location, in which size S_A expressed in squared kilometers, depends on the magnitude of the mainshock according to the model of Utsu (1970):

$$S_A = 10^{m-4.1}. \tag{5}$$

Alternative models for the shape of the area enclosing aftershocks can be found in literature (e.g., Kanamori and Anderson, 1975) and could be equivalently used in SPSHA. An interesting approach is that of Zhuang *et al.* (2002), who model the probability distribution of aftershocks location with a bell-shape decay from the mainshock location, yet they discuss that such a model relies on the same understanding as that in Utsu (1970). Thus, it is expected that selecting an alternative model for the shape of the area enclosing aftershocks does not significantly affect the results. Finally, for the hazard analyses the duration of the aftershock sequence, ΔT_A, was

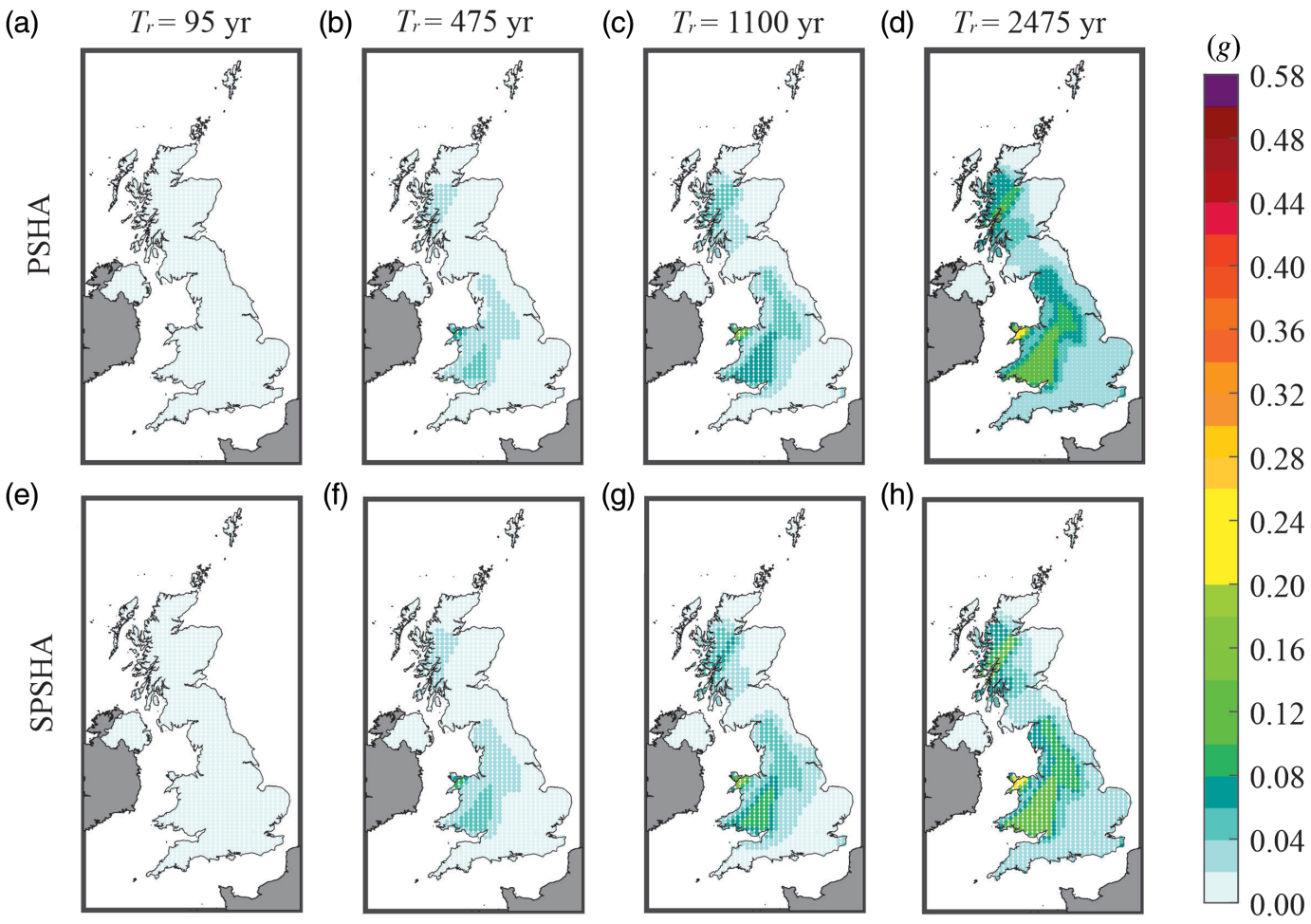

Figure 4. Maps of *PGA* on rock with $T_r = 95$ yr, $T_r = 475$ yr, $T_r = 1100$ yr, and $T_r = 2475$ yr, from left to right, obtained using PSHA (a–d) and sequence-based PSHA (SPSHA; e–h).

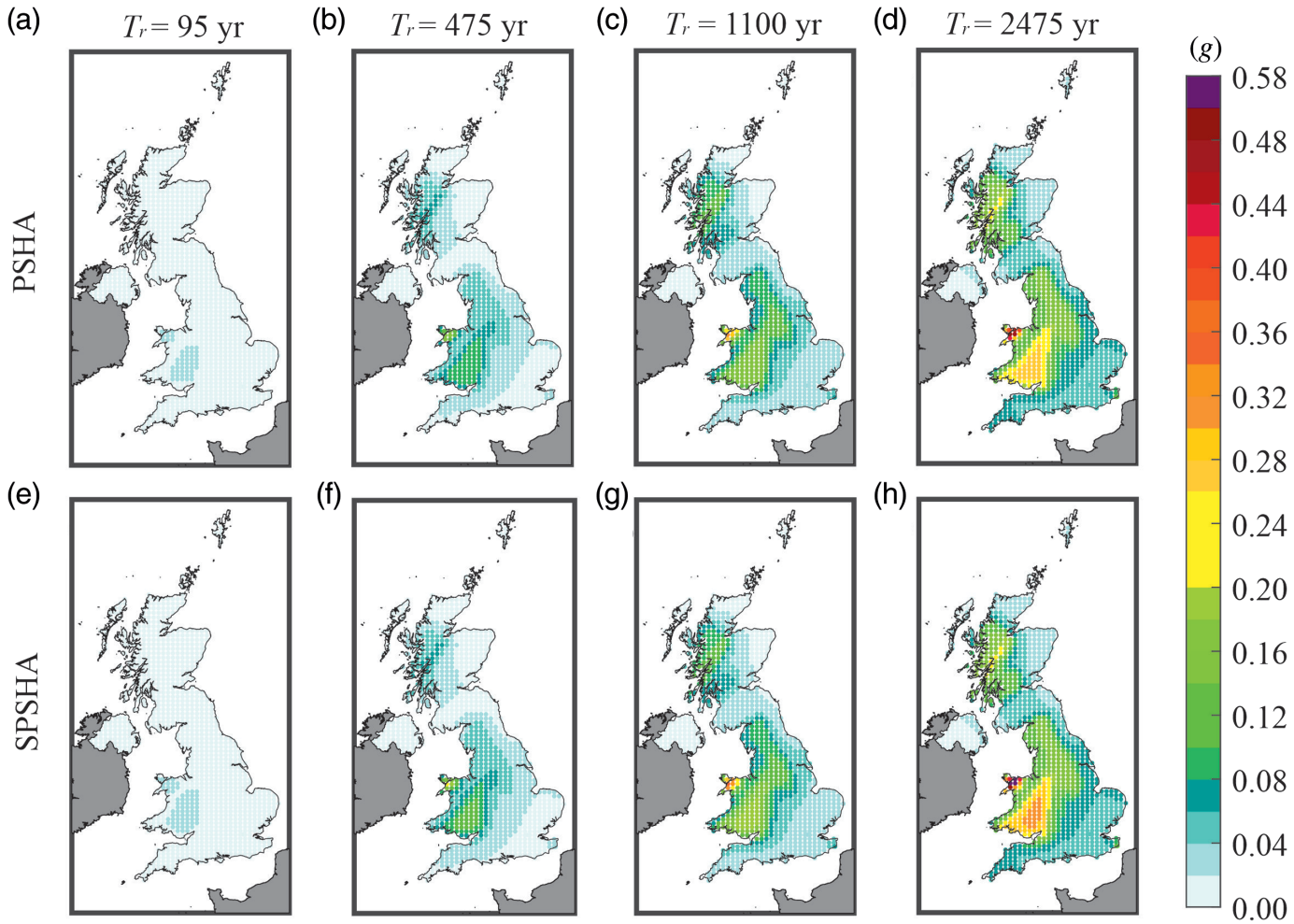

Figure 5. Maps of $Sa(T = 0.2$ s) on rock with $T_r = 95$ yr, $T_r = 475$ yr, $T_r = 1100$ yr, and $T_r = 2475$ yr, from left to right, obtained using PSHA (a–d) and SPSHA (e–h).

assumed arbitrarily equal to 90 days from the occurrence of the mainshock, although, in principle, this duration could be mainshock magnitude dependent. This assumption is consistent with the other studies applying SPSHA (Iervolino *et al.*, 2018; Chioccarelli *et al.*, 2021); nevertheless, it has been observed that the Omori law's parameters calibrated for the UK renders the results of hazard analysis slightly more dependent on ΔT_A than the previous studies (see Sensitivity analysis section).

ANALYSIS AND RESULTS

The analyses were carried out through the REASSESS software (Chioccarelli *et al.*, 2019), in which the simplified source model for the UK was implemented (and made available for eventual further studies). PSHA and SPSHA hazard curves, in terms of *PGA*, $Sa(T = 0.2$ s), and $Sa(T = 1.0$ s), were computed for more than four thousand sites across the country, which are the nodes of a regular grid spacing 0.250° and 0.125° longitude and latitude, respectively.

Hazard maps

PSHA and SPSHA results for any site in the UK are represented in Figure 4 for *PGA*, and in Figures 5 and 6 for $Sa(T = 0.2$ s) and $Sa(T = 1.0$ s), respectively. In each figure, the panels from (a) to (d) show the spectral ordinate that the figure refers with exceedance return period from 95 yr to 2475 yr, according to PSHA; panels from (e) to (h) represent the results when mainshock–aftershock sequences are taken into account in SPSHA.

Looking at the figures, it can be observed that sites with the highest hazard are located in the western UK for each spectral and exceedance return period, that is, in the area enclosing the seismic zones EISB, MENA, BALA, and MMCW. This area also includes the sites exposed to the largest sequence-based seismic hazard, according to the bottom panels. This is somehow expected, as the more frequent and stronger (in terms of magnitude) the mainshocks the larger the number of expected aftershocks. The largest *PGA*, which is exceeded once every 2475 yr (on average) due to mainshocks–aftershocks sequences, is equal to 0.272*g*; for the same return period, the largest values for $Sa(T = 0.2$ s) and $Sa(T = 1.0$ s) across the country are

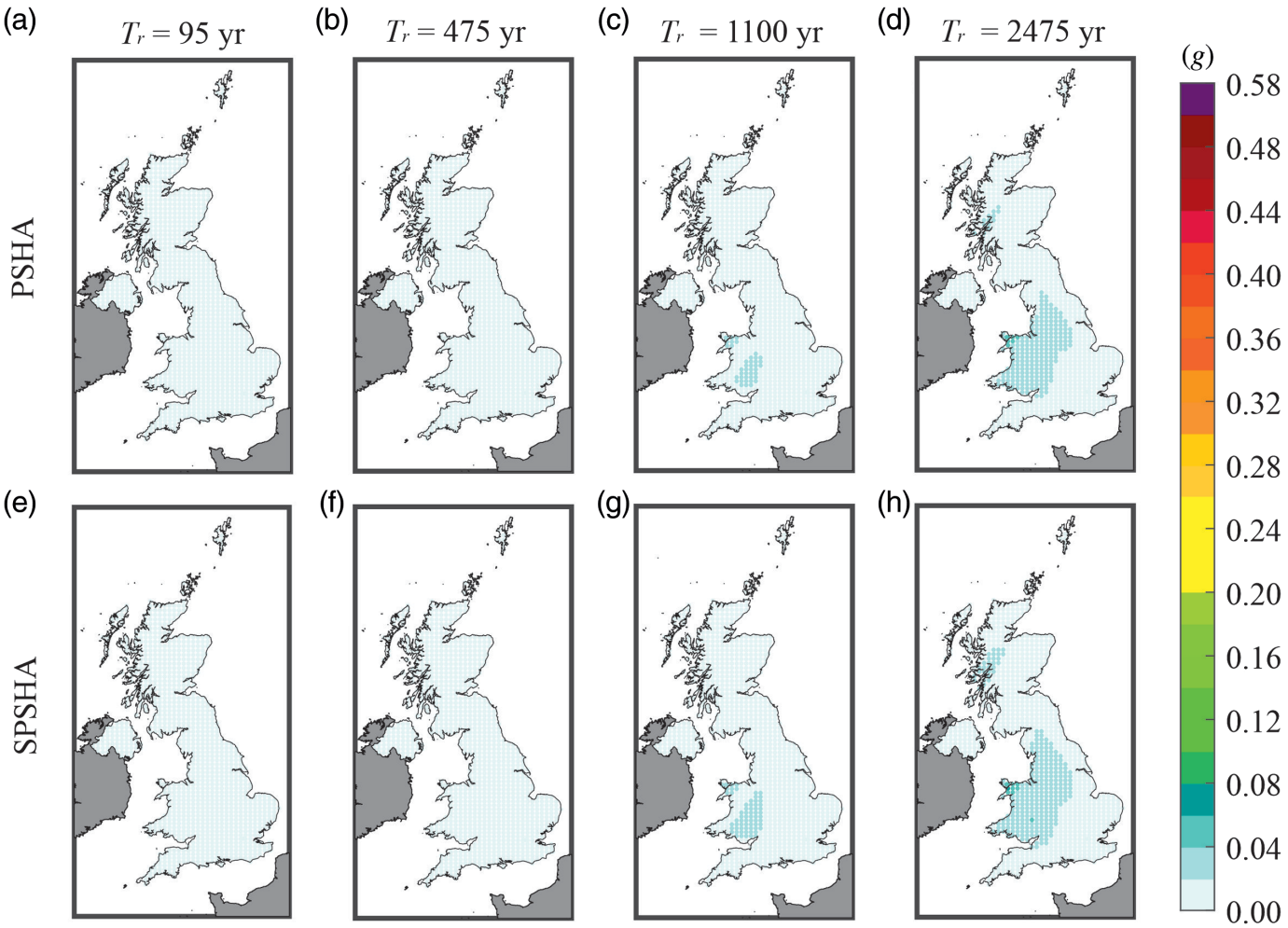

Figure 6. Maps of $Sa(T = 1.0\ s)$ on rock with $T_r = 95$ yr, $T_r = 475$ yr, $T_r = 1100$ yr, and $T_r = 2475$ yr, from left to right, obtained using PSHA (a–d) and SPSHA (e–h).

0.564*g* and 0.061*g*, respectively. The sites with the lowest hazard are enclosed by the ESCO zone in the northeastern area of the UK. For example, in proximity of Aberdeen (2.1° W, 57.16° N), a *PGA* value of 0.012*g* is exceeded, on average, once every 2475 yr, even considering the aftershock effects; for the same return period, the lowest ground-motion intensity at the same site is equal to 0.022*g* for $Sa(T = 0.2\ s)$ and 0.008*g* for $Sa(T = 1.0\ s)$. The southeast area of the UK is exposed to relatively moderate seismic hazard. For example, at the site of Norwich (1.30° E, 52.63° N), the largest *PGA*, $Sa(T = 0.2\ s)$, and $Sa(T = 1.0\ s)$ for $T_r = 2475$ yr using SPSHA are equal to 0.031*g*, 0.0606*g*, and 0.013*g*, respectively.

It appears that the hazard increase due to aftershocks is not the same across the country. This is not unexpected, as the magnitude and number of aftershocks increase with seismic hazard due to mainshocks (see also Iervolino *et al.*, 2018; Chioccarelli *et al.*, 2021). Moreover, results reveal that aftershocks effect varies with the exceedance return period and spectral ordinate, as discussed in the following. To analyze quantitatively the results, Figure 7 shows the distributions of the differences between SPSHA and PSHA results across the country, computed at each site as $sa_{SPSHA} - sa_{PSHA}$; dividing this difference by sa_{PSHA} gives the relative hazard increases due to aftershocks, relatively to PSHA results (Fig. 8), that is, $(sa_{SPSHA} - sa_{PSHA})/sa_{PSHA}$. In both the figures, panels (a–d), (e–h), and (i–l) refer to *PGA*, $Sa(T = 0.2\ s)$, and $Sa(T = 1.0\ s)$, respectively; in each row, panels from left to right show the differences for exceedance return periods from 95 yr to 2475 yr.

As already mentioned, for each spectral ordinate and exceedance return period, it can be observed that aftershocks effect tends to increase (decrease) as the seismic hazard increases (decreases) according to classical PSHA, in both absolute and relative terms. Looking at the figures vertically, for each return period, the trend of the differences is the same as that of hazard results with the vibration period, which depends on the GMPE, that is, it is comparatively larger at the low vibration periods. In fact, according to the maps, the maximum differences over the whole country are observed for $Sa(T = 0.2\ s)$, whereas the lowest are recorded for $Sa(T = 1.0\ s)$; differences in terms of *PGA* are in intermediate situation. On average, over the country, the absolute difference

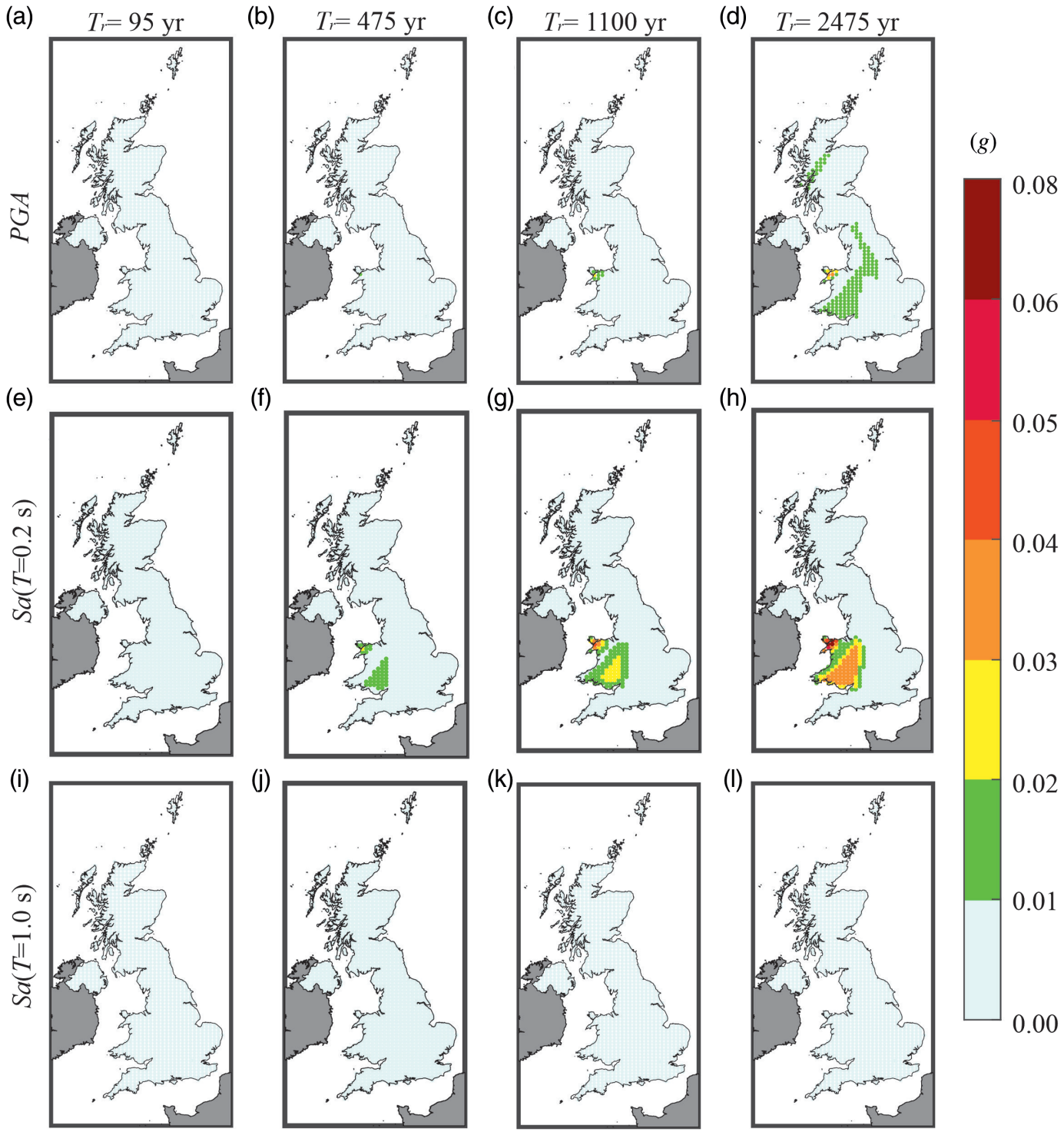

ranges from $3.88 \times 10^{-04}g$, for $T_r = 95$ yr, to $0.005g$, for $T_r = 2475$ yr, for *PGA*, whereas they are $3.77 \times 10^{-04}g$ and $0.004g$ for $T_r = 95$ yr and $T_r = 2475$ yr, respectively, for $Sa(T = 0.2$ s); for $Sa(T = 1.0$ s), increments are very low, being about $0.001g$, on average, for the largest return period (see Table 3). Considering the ensemble of the return periods discussed so far, the average relative increments over the country are within 10.2% and 10.9% for *PGA*, 2.4% and 3.2% for $Sa(T = 0.2$ s), and 8.3% and 9.6% for $Sa(T = 1.0$ s).

Figure 7. Absolute differences between SPSHA and PSHA results in terms of (a–d) peak ground acceleration (*PGA*), (e–h) $Sa(T = 0.2$ s), and (i–l) $Sa(T = 1.0$ s), with $T_r = 95$ yr, $T_r = 475$ yr, $T_r = 1100$ yr, and $T_r = 2475$ yr, from left to right.

For each spectral ordinate, one can observe that absolute differences tend to increase with increasing the return period. However, the largest increment over the country, in absolute

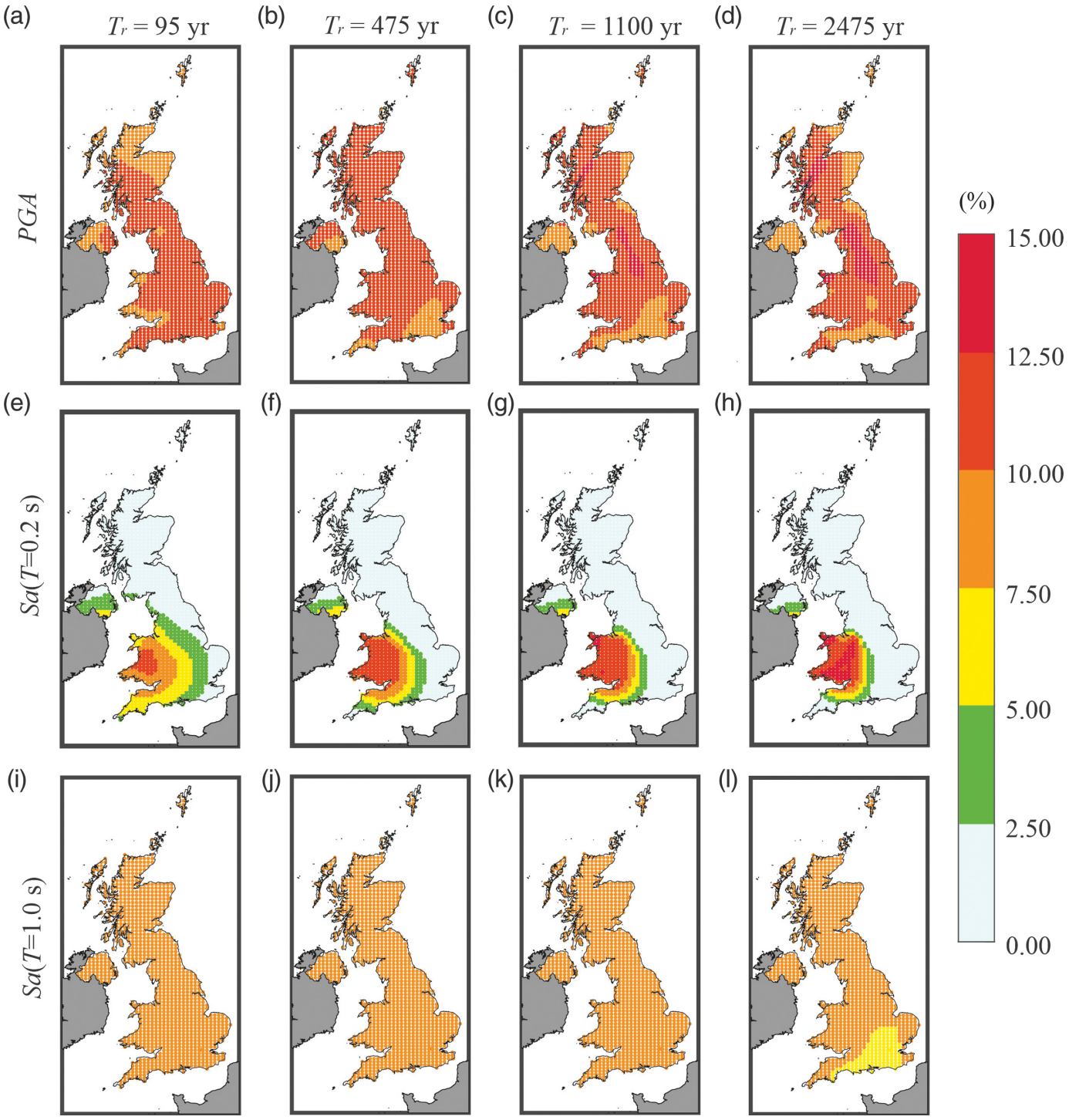

terms, is well below 0.1*g*. Looking at the map in Figure 7, it is found that, in proximity of the high hazardous MENA zone, the difference between SPSHA and PSHA results, in terms of $Sa(T = 0.2\text{ s})$ with $T_r = 2475$ yr, is equal to 0.069*g*. Given the spectral ordinate, the trend of the relative increments as a function of the return period is nonmonotonic. The largest percentage difference is found for $T_r = 2475$ yr in the case of *PGA* (north England) and $Sa(T = 0.2\text{ s})$ (northwest Wales), being about 13.8% in both the cases, whereas, for $Sa(T = 1.0\text{ s})$, it is about 10% (western Scotland) for $T_r = 1100$ yr. To summarize the results represented in Figures 7 and 8, the average and maximum differences in both absolute and relative terms are given in Table 3 for each spectral and exceedance return period.

Figure 8. Relative differences between SPSHA and PSHA results in terms of (a–d) *PGA*, (e–h) $Sa(T = 0.2\text{ s})$, and (i–l) $Sa(T = 1.0\text{ s})$, with $T_r = 95$ yr, $T_r = 475$ yr, $T_r = 1100$ yr, and $T_r = 2475$ yr, from left to right.

TABLE 3
Average and Maximum Difference in Absolute and Relative Terms of Sequence-Based Probabilistic Seismic Hazard Analysis (SPSHA) Results with Respect to PSHA Counterparts

	PGA				*Sa*(T = 0.2s)				*Sa*(T = 1.0s)			
T_r(yr)	95	475	1100	2475	95	475	1100	2475	95	475	1100	2475
Average percentage difference (%)	10.2	10.7	10.8	10.9	3.2	2.9	2.7	2.4	9.2	9.6	9.1	8.3
Average absolute difference (g)	3.88×10^{-04}	0.0016	0.0030	0.0051	3.77×10^{-04}	0.0015	0.0026	0.0041	1.18×10^{-04}	4.99×10^{-04}	8.52×10^{-04}	0.0013
Maximum percentage difference (%)	10.9	12.2	13.2	13.8	10.8	12.2	13.5	13.8	9.8	9.9	10.0	9.9
Maximum absolute difference (g)	0.001	0.010	0.020	0.033	0.003	0.022	0.043	0.069	2.72×10^{-04}	0.002	0.003	0.006

PGA is peak ground acceleration; *Sa*(T = 0.2 s) is the spectral accelerations at 0.2 s natural vibration period; *Sa*(T = 1.0 s) is the spectral accelerations at 1.0 s natural vibration period; and T_r is the return period.

To close this section, the aftershock effects on design seismic actions discussed so far are briefly compared to those estimated for Italy by Iervolino *et al.* (2018). Because of the larger seismic hazard, it is expected that aftershock effects in Italy (see figs. 2 and 3 in Iervolino *et al.*, 2018) are more significant, both in relative and absolute terms, than those for the UK. For example, considering *PGA* and the largest return period (T_r = 2475 yr) for the most hazardous sites, the relative increment in Italy (about 28%) can be even twice that found for the UK (about 14%). Still with reference to *PGA* and T_r = 2475 yr, the largest absolute difference between SPSHA and PSHA results are equal to 0.116g and 0.033g for Italy and the UK, respectively. Such a difference is also related to the fact that, for the same return period, spectral accelerations according to PSHA for the UK are lower than the Italian counterparts, yet by a larger ratio. More precisely, in the most hazardous areas of Italy, *PGA* for T_r = 2475 yr (about 0.6g) is almost three times the largest *PGA* (for the same return period) for the UK (about 0.25g).

Site-specific hazard analysis

In the Hazard maps section it has been shown that aftershock effects on design seismic actions depend on the seismic hazard of the site, the spectral and exceedance return period. Now, SPSHA and PSHA results are discussed in more detail for the sites of Edinburgh (3.19° W, 55.95° N), Cardiff (3.18° W, 51.49° N), and Llangefni (4.31° W, 53.25° N). They were selected because representative of comparatively low, medium, and high hazard level across the country according to PSHA, respectively. The location of the considered sites is shown in Figure 1. The aim is to (1) investigate the increase in seismic hazard due to aftershocks with respect to an interval of spectral and return periods larger than those considered in the Hazard maps section and (2) to give insights on the differences between PSHA- and SPSHA-based hazard results.

PSHA and SPSHA results for the sites are compared in Figure 9. The columns, each referring to a site, are ordered following the increasing seismic hazard, from left to right. Panels from (a) to (c) represent the hazard curves in terms of *PGA*, *Sa*(T = 0.2 s), and *Sa*(T = 1.0 s) according to PSHA (gray lines) and SPSHA (black lines). Panels from (d) to (f) show the UHS obtained from PSHA (gray lines) and SPSHA (black lines) for the return periods considered before. The spectral ordinates were computed considering 24 natural vibration periods, which are those used in the GMPE of Bindi *et al.* (2014). Based on the UHS, the relative hazard increments, as defined in the Hazard maps section, are represented in panels from (g) to (i), for each *Sa*(T) and exceedance return period. In addition, the effect of aftershocks on the hazard, in terms of *PGA*, *Sa*(T = 0.2 s), and *Sa*(T = 1.0 s) as a function of return period from 50 yr to 10,000 yr is shown in panels from (j) to (l). Looking at the figure, it can be observed that the largest hazard increases are for the low-to-mid vibration periods (i.e., lower than 0.3 s),

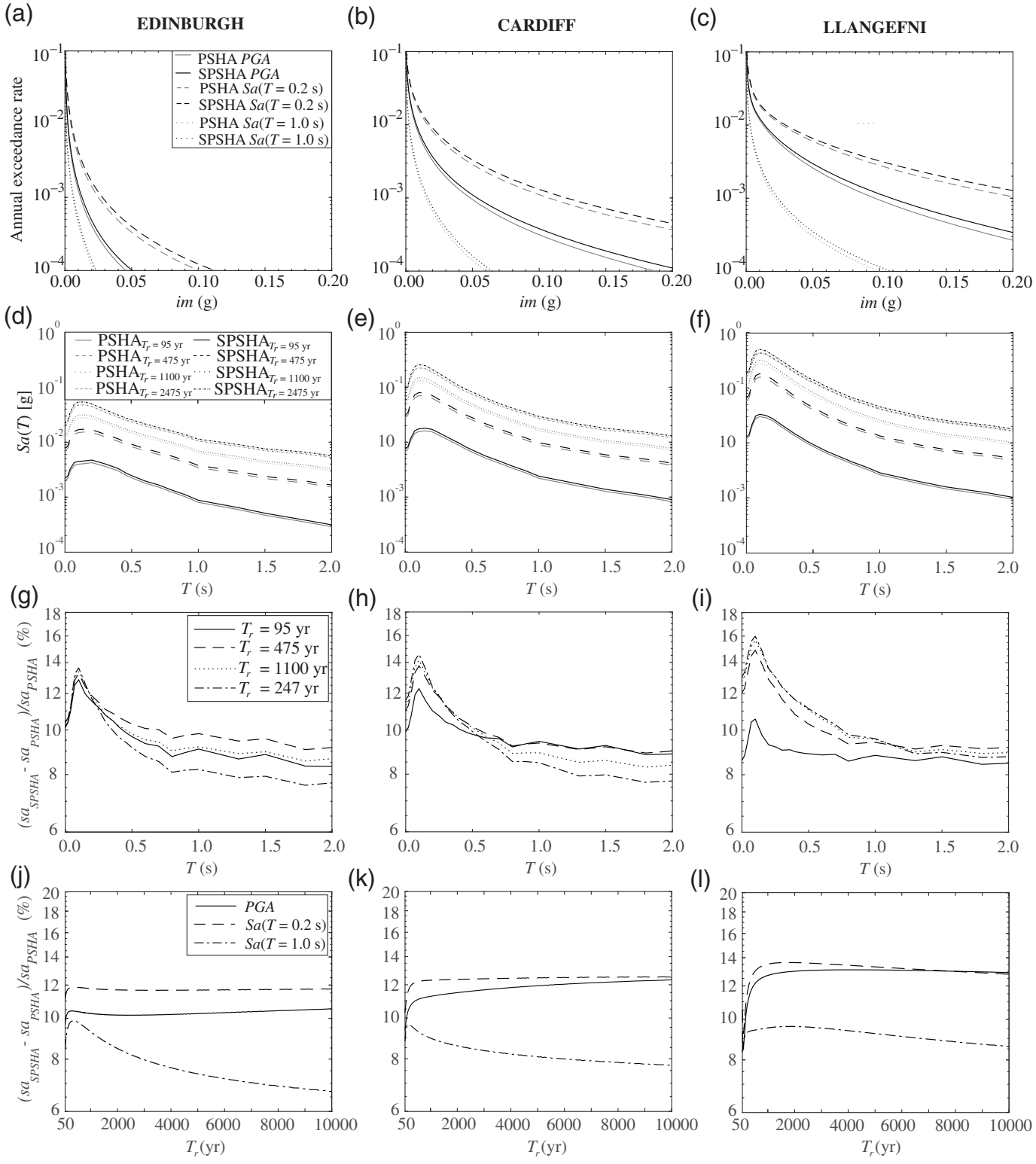

Figure 9. Results of hazard analysis for the three sites of interest: hazard curves in terms of *PGA*, $Sa(T = 0.2\text{ s})$, and $Sa(T = 1.0\text{ s})$ for the site of (a) Edinburgh, (b) Cardiff, and (c) Llangefni; UHS with $T_r = 95$ yr, $T_r = 475$ yr, $T_r = 1100$ yr, and $T_r = 2475$ yr, for the site of (d) Edinburgh, (e) Cardiff, and (f) Llangefni; relative hazard increase as function of the spectral period for four T_r values for the site of (g) Edinburgh, (h) Cardiff, and (i) Llangefni; relative hazard increase as function of T_r in terms of *PGA*, $Sa(T = 0.2\text{ s})$, and $Sa(T = 1.0\text{ s})$ for the site of (j) Edinburgh, (k) Cardiff, and (l) Llangefni.

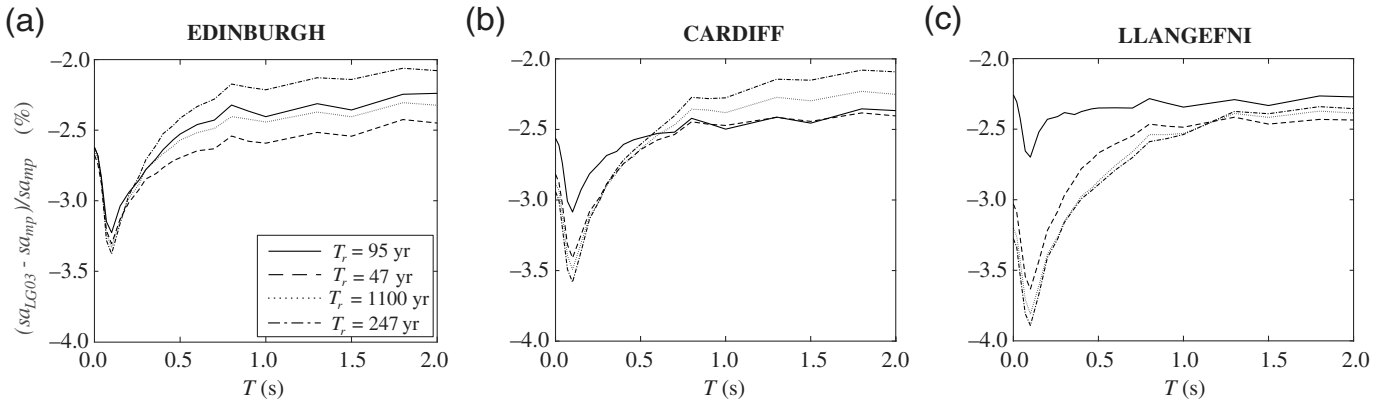

Figure 10. Comparison of UHS obtained from hazard analysis conducted using the parameters of Lolli and Gasperini (2003), sa_{LG03}, and those obtained from hazard analysis conducted using the mean parameters calibrated for the UK, sa_{mp}, for the site of (a) Edinburgh, (b) Cardiff, and (c) Llangefni.

independently on the seismic hazard of the site and the considered exceedance return period. At each site, the largest relative differences are for the vibration period equal to 0.1 s and all the return periods; more specifically, they are 13.6%, 14.6%, and 16% for Edinburgh, Cardiff, and Llangefni, respectively. Panels from (g) to (i) also show that, considering the long vibration periods (i.e., larger than 1.0 s), the hazard increments at each site are lower than those found at the short periods and are almost constant. In fact, considering the return periods from 95 yr to 2475 yr, they range from about 7.5% to 10% for both Edinburgh and Cardiff, whereas they are around 9% for any return period in the case of Llangefni. This reveals that the contribution of aftershocks to seismic hazard tends to decrease with the increase of the spectral period independently of the seismic hazard of the site and the exceedance return period; see Iervolino *et al.* (2018) and Chioccarelli *et al.* (2021) for a discussion on this issue.

Panels from (g) to (i) confirm that the relative increment in the design seismic actions due to aftershocks with respect to PSHA results does not monotonically increase with the return period. For example, for $Sa(T = 0.1$ s), it can be observed that the largest difference is found for $T_r = 475$ yr in the case of Edinburgh, whereas it is for $T_r = 2475$ yr for the other two sites. Thus, one may be interested in exploring the trend of the hazard increment in a range of return periods wider than that considered so far. To do this, one should look at panels from (j) to (l). They reveal that, at each site, the increments increase in a very limited range of return periods and tend to flatten out at T_r values larger than 4000 yr (and up to the largest herein considered) in the case of *PGA* and $Sa(T = 0.2$ s), whereas, for $Sa(T = 1.0$ s), they monotonically decrease for return periods from 2000 yr onward. This is expected from the disaggregation of sequence-based seismic hazard (i.e., Chioccarelli *et al.*, 2018), according to which the contribution of aftershocks to hazard as a function of T_r is not the same at the different vibration periods. For Edinburgh, the maximum increments for *PGA*, $Sa(T = 0.2$ s), and $Sa(T = 1.0$ s) are about 10.5%, 11.9%, and 9.9%, respectively. They occur at different return periods, being $T_r = 9980$ yr for *PGA*, $T_r = 470$ yr for $Sa(T = 0.2$ s), and $T_r = 360$ yr for $Sa(T = 1.0$ s). Considering the site of Cardiff, the maximum increases in terms of *PGA*, $Sa(T = 0.2$ s) and $Sa(T = 1.0$ s) are equal to 12.3%, 12.5%, and 9.6%, and they occur at return periods of 9990 yr, 9690 yr, and 170 yr, respectively. Finally, for Llangefni, the maximum percentage difference between SPSHA and PSHA results in terms of *PGA* is equal to 13.1%, and it is observed for $T_r = 4060$ yr; in the case of $Sa(T = 0.2$ s), the largest difference is similar to that for *PGA*, being equal to 13.6%, but it is found for $T_r = 1720$ yr; looking at the trend for $Sa(T = 1.0$ s), the peak, which is equal to 9.6%, occurs at $T_r = 1830$ yr.

Sensitivity analysis. Because the paucity of seismic sequences led to a simplified calibration of the modified Omori law parameters, this section deals with some sensitivity analysis of the results to such parameters, that is, $\{a, c, p\}$, also including ΔT_A.

First, the UHS derived via the SPSHA based on the mean parameters (*mp*) obtained herein $\{a = -1.71, c = 0.0023, p = 0.68\}$, that is, the spectra in panels from (d) to (f) of Figure 9, are compared to those obtained using $\{a = -1.66, c = 0.0295, p = 0.93\}$, which are the more consolidated parameters fitted, using forty seismic sequences occurred in Italy, by Lolli and Gasperini (2003); hereafter, *LG*03. The comparison is given in Figure 10 that, for the three sites considered in the Site-Specific Hazard Analysis section, provides the relative differences between the spectral ordinates obtained using the *LG*03 parameters with respect to the counterparts obtained using the *mp* set, that is, $(sa_{LG03} - sa_{mp})/sa_{mp}$, for four return periods. The differences are limited, being them in the range between 1.8% and 3.9% overall. On one hand, this shows that, even using the parameters calibrated on a dataset larger than

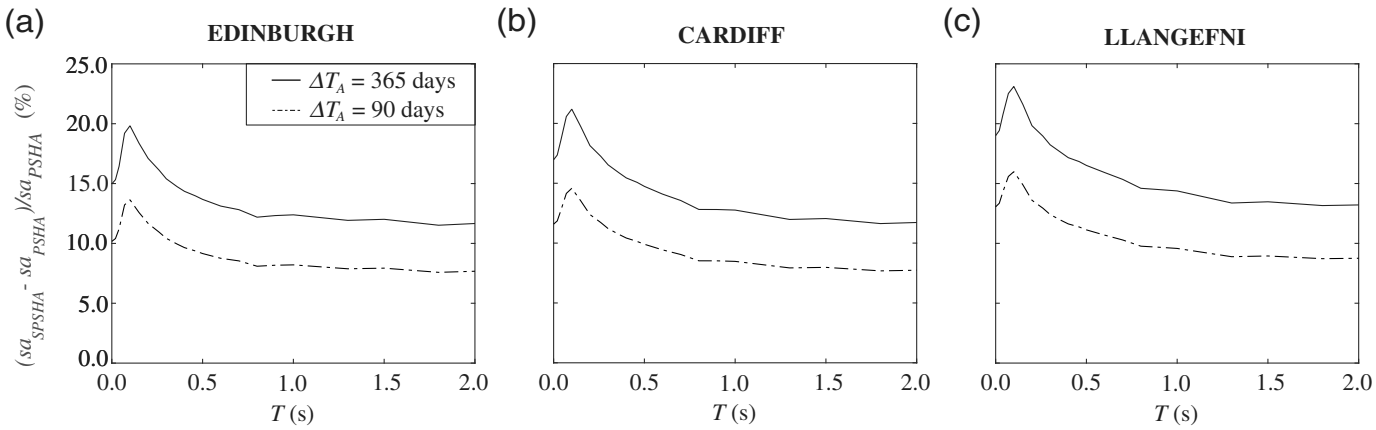

Figure 11. Comparison of UHS with $T_r = 2475$ yr obtained from hazard analysis conducted using the mean parameters calibrated for the UK with $\Delta T_A = 90$ days and $\Delta T_A = 365$ days for the site of (a) Edinburgh, (b) Cardiff, and (c) Llangefni.

the one used in this study, the SPSHA results do not significatively change, something that, in turn, may suggest that fitting {*a*, *c*, *p*} via a more refined procedure does not necessarily turn into relevant differences in terms of sequence-based hazard maps. On the other hand, this sensitivity analysis only deals with the implications of the parameter choices on the hazard results and does not solve the paucity of data for UK, which may have affected the estimation of the modified Omori law parameters, as already discussed. Moreover, it has the intrinsic limit that the two considered {*a*, *c*, *p*} sets are fitted on data from countries with generally different seismicity. However, the sensitivity of results to Omori parameters is deepened in Orlacchio *et al.* (2022).

Finally, considering the 2475 yr UHS for the sites of Edinburgh, Cardiff, and Llangefni, Figure 11 shows the sensitivity of the relative hazard increase, with respect to PSHA results, to the ΔT_A interval assumed in the analysis. It is shown that varying ΔT_A from 90 to 365 days does not significantly affect the results.

CONCLUSIONS

For reasons mainly related to the ease of calibration and use, implied by the homogeneous Poisson process assumption for earthquake occurrence and the limited completeness of information about foreshocks and aftershocks in seismic catalogs, classical PSHA only considers mainshocks in determining the rate of seismic events that exceed a ground motion intensity at a site of interest. However, sequence-based probabilistic seismic hazard analysis allows us to account for the effect of aftershocks in the hazard assessment, keeping the same advantages of PSHA. In fact, SPSHA still resources from a declustered catalog and assumes the homogeneous Poisson process assumption for the occurrence of mainshock–aftershocks sequences. Finally, SPSHA relies on an analytical formulation that is relatively easy to implement. Moreover, literature recently discussed that it is in good agreement with other seismic sequences modeling approaches, generally more cumbersome in calibration and simulation.

In the presented study, SPSHA was applied to investigate the hazard increase due to aftershocks in the UK, using the recent source model from the BGS. The parameters of the modified Omori law, which was used to model aftershock occurrence, were calibrated in a simplified manner based on four seismic sequences occurred in the UK (no more than that due to paucity of quality data), assumed to be complete in the magnitude range of interest. A very simple sensitivity analysis was carried out to assess the effects of the modified Omori law parameters on the results. It was verified that using parameters for a relatively high-seismicity country, such as Italy, does not lead to relevant differences in the hazard results.

Considering four exceedance return periods of interest to structural engineering from 95 yr to 2475 yr, hazard maps, in terms of *PGA*, $Sa(T = 0.2$ s), and $Sa(T = 1.0$ s), resulting from SPSHA, were computed for rock site conditions, and compared to the PSHA counterparts based on the same source model and GMPE. Moreover, with reference to the three sites, the PSHA and SPSHA results for exceedance return periods up to 10,000 yr and 24 spectral ordinates were compared and discussed in greater detail to give further insights about the aftershock implications. Finally, the aftershock effects estimated for the UK were briefly compared to a previous SPSHA study for Italy, a relatively larger seismic hazard country. Some remarks that can be drawn from the results are listed in the following.

- For each spectral and return period, the hazard increase tends to be more relevant in the areas covering most of Wales, north central England, and western Scotland.
- For a given spectral ordinate, the largest percentage increase due to aftershocks over the country has a nonmonotonic trend with the return period; the largest value across the country, equal to 10%, was found at $T_r = 1100$ yr for $Sa(T = 1.0$ s), whereas it is 14% at $T_r = 2475$ yr for *PGA* and $Sa(T = 0.2$ s).
- For a given spectral ordinate, the maximum absolute differences between SPSHA and PSHA results over the country monotonically increase with return period (in the

range considered). Nationwide, for $T_r = 2475$ yr, the largest difference between SPSHA and PSHA are equal to 0.033*g*, 0.069*g*, and 0.006*g* for *PGA*, $Sa(T = 0.2$ s), and $Sa(T = 1.0$ s), respectively.

- On average across the country, the absolute differences, for $T_r = 2475$ yr, are equal to 0.0051*g*, 0.0041*g*, and 0.0013*g* for *PGA*, $Sa(T = 0.2$ s), and $Sa(T = 1.0$ s), respectively.
- Considering the range of return periods between 95 yr and 2475 yr, the largest average percentage differences are equal to 11% in the case of *PGA*, 3% for $Sa(T = 0.2$ s), and 10% for $Sa(T = 1.0$ s); they were found at $T_r = 2475$ yr, $T_r = 95$ yr, and $T_r = 475$ yr, respectively.
- The analysis for specific sites revealed that the aftershock effects are more significant at vibration periods lower than 0.3 s and tend to decrease for those larger, becoming almost constant from 1.0 s onward. The largest relative difference between SPSHA and PSHA results was found at 0.1 s for all the sites. With reference to Llangefni, which is the site characterized by the highest seismic hazard countrywide, the return period for which the largest hazard increase is found significantly varies among the different spectral ordinates, being equal to 4060 yr, 1720 yr, and 1830 yr for *PGA*, $Sa(T = 0.2$ s), and $Sa(T = 1.0$ s), respectively.
- In the most hazardous sites of the UK, the hazard percentage increments of SPSHA results with respect to PSHA are about half than those found in the most hazardous areas of Italy, although in Italy the larger spectral acceleration associated to a given return period can be three times larger than the analogous one in the UK.

DATA AND RESOURCES

All data and resources used in this study came from published sources listed in the references. The supplemental material includes the hazard maps resulting from the study herein discussed.

DECLARATION OF COMPETING INTEREST

The authors acknowledge that there are no conflicts of interest recorded.

ACKNOWLEDGMENTS

The study was developed within the activities of the Ph.D. program "PON Ricerca e Innovazione 2014-2020 (CCI 2014IT16M2OP005) Fondo Sociale Europeo, Azione I.1, Dottorati Innovativi con caratterizzazione Industriale". The authors want to thank Mosca I., Sargeant, B. Baptie, R.M.W. Musson, and T. Pharaoh who have kindly provided the results of the British Geological Survey (BGS) study. The anonymous reviewers and the associate editor, who helped to improve the quality of the article, are also gratefully acknowledged.

REFERENCES

Atkinson, G. M., and D. M. Boore (2006). Earthquake ground-motion prediction equations for eastern North America, *Bull. Seismol. Soc. Am.* **96,** no. 6, 2181–2205.

Atkinson, G. M., and D. M. Boore (2011). Modifications to existing ground-motion prediction equations in light of new data, *Bull. Seismol. Soc. Am.* **101,** no. 3, 1121–1135.

Atik, L. A., A. Kottke, N. Abrahamson, and J. Hollenback (2014). Kappa (κ) scaling of ground-motion prediction equations using an inverse random vibration theory approach, *Bull. Seismol. Soc. Am.* **104,** no. 1, 336–346.

Bindi, D., M. Massa, L. Luzi, G. Ameri, F. Pacor, R. Puglia, and P. Augliera (2014). Pan-European ground-motion prediction equations for the average horizontal component of PGA, PGV, and 5%-damped PSA at spectral periods up to 3.0 s using the RESORCE dataset, *Bull. Earthq. Eng.* **12,** no. 1, 391–430.

Boore, D. M., J. Stewart, E. Seyhan, and G. M. Atkinson (2014). NGA-West2 equations for predicting PGA, PGV, and 5% damped PSA for shallow crustal earthquakes, *Earthq. Spectra* **30,** 1057–1085.

British Geological Survey (BGS) (2020). National seismic hazard maps for the UK: 2020 update, *Open Rept. OR/20/053*, 86 pp.

Cauzzi, C., E. Faccioli, M. Vanini, and A. Bianchini (2015). Updated predictive equations for broadband (0.01–10 s) horizontal response spectra and peak ground motions, based on a global dataset of digital acceleration records, *Bull. Earthq. Eng.* **13,** no. 6, 1587–1612.

Chioccarelli, E., P. Cito, and I. Iervolino (2018). Disaggregation of sequence-based seismic hazard, *Proc. of the 16th European Conf. Earthquake Engineering*, Thessaloniki, Greece, 18–21 June 2018.

Chioccarelli, E., P. Cito, I. Iervolino, and M. Giorgio (2019). REASSESS V2.0: Software for single- and multi-site probabilistic seismic hazard analysis, *Bull. Earthq. Eng.* **17,** no. 4, 1769–1793.

Chioccarelli, E., P. Cito, F. Visini, and I. Iervolino (2021). Sequence-based hazard analysis for Italy considering a grid seismic source model, *Ann. Geophys.* doi: 10.4401/ag-8586.

Cornell, C.A. (1968). Engineering seismic risk analysis, *Bull. Seismol. Soc. Am.* **58,** 1583–1606.

Cotton, F., F. Scherbaum, J. J. Bommer, and H. Bungum (2006). Criteria for selecting and adjusting ground-motion models for specific target regions: Application to central Europe and rock sites, *J. Seismol.* **10,** no. 2, 137–156.

Gardner, J. K., and L. Knopoff (1974). Is the sequence of earthquakes in southern California, with aftershocks removed, Poissonian? *Bull. Seismol. Soc. Am.* **64,** no. 5, 1363–1367.

Gutenberg, B., and C. F. Richter (1944). Frequency of earthquakes in California, *Bull. Seismol. Soc. Am.* **64,** no. 5, 185–188.

Hardebeck, J.L., A. L. Llenos, A. J. Michael, M. T. Page, and N. van der Elst (2018). Updated California aftershock parameters, *Seismol. Res. Lett.* **90,** no. 1, 262–270.

Helmstetter, A. (2003). Is earthquake triggering driven by small earthquakes? *Phys. Rev. Lett.* **91,** no. 5, 3–6.

Iervolino, I. (2016). Soil-invariant seismic hazard and disaggregation, *Bull. Seismol. Soc. Am.* **106,** no. 4, 1900–1907.

Iervolino, I., E. Chioccarelli, and M. Giorgio (2018). Aftershocks' effect on structural design actions in Italy, *Bull. Seismol. Soc. Am.* **108,** no. 4, 2209–2220.

Iervolino, I., M. Giorgio, and B. Polidoro (2014). Sequence-based probabilistic seismic hazard analysis, *Bull. Seismol. Soc. Am.* **104,** no. 2, 1006–1012.

Joyner, W. B., and D. M. Boore (1981). Peak horizontal acceleration and velocity from strong-motion records including records from

the 1979 Imperial valley, California, earthquake, *Bull. Seismol. Soc. Am.* **71,** no. 6, 2011–2038.

Kanamori, H., and D. L. Anderson (1975). Theoretical basis of some empirical relations in seismology, *Bull. Seismol. Soc. Am.* **65,** no. 5, 1073–1095.

Kramer, S. L. (1996). *Geotechnical Earthquake Engineering*, Prentice-Hall, New Jersey.

Kutoyantis, Y. A. (1982). Multidimensional parameter estimation of the intensity function of inhomogeneous Poisson processes, *Control Inform. Theor.*, **11,** no. 4, 325–334.

Lolli, B., and P. Gasperini (2003). Aftershocks hazard in Italy part I: Estimation of time-magnitude distribution model parameters and computation of probabilities of occurrence, *J. Seismol.* **7,** no. 2, 235–257.

Marzocchi, W., and M. Taroni (2014). Some thoughts on declustering in probabilistic seismic-hazard analysis, *Bull. Seismol. Soc. Am.* **104,** no. 4, 1838–1845.

McGuire, R. K. (2004). *Seismic hazard and risk analysis*, Earthquake Engineering Research Institute Publication, Rept. MNO-10, Oakland, California, 221 pp.

Montaldo, V., E. Faccioli, G. Zonno, A. Akinci, and L. Malagnini (2005). Treatment of ground-motion predictive relationships for the reference seismic hazard map of Italy, *J. Seismol.* **9,** no. 3, 295–316.

Mosca, I., S. Sargeant, B. Baptie, R. M. W. Musson, and T. Pharaoh (2022). The 2020 national seismic hazard model for the United Kingdom, *Bull. Earthq. Eng.* **20,** 633–675.

Ogata, Y. (1978). The asymptotic behaviour of the maximum likelihood estimators for the stationary point processes, *Ann. Inst. Stat. Math.* **30,** 243–261.

Ogata, Y. (1983). Estimation of the parameters in the modified Omori formula for aftershock frequencies by the maximum likelihood procedure, *J. Phys. Earth*, **31,** no. 2, 115–124.

Ogata, Y. (1988). Statistical models for earthquake occurrences and residual analysis for point processes, *J. Am. Stat. Assoc.* **83,** no. 401, 9–27.

Orlacchio, M., P. Cito, and I. Iervolino (2022). A sensitivity analysis of sequence-based seismic hazard assessment for the United Kingdom, *3rd European Conf. Earthquake Engineering and Seismology*, Bucarest, Romania, 4–9 September 2022.

Page, M. T., N. van Der Elst, J. Hardebeck, K. Felzer, and A. J. Michael (2016). Three ingredients for improved global aftershock forecasts: Tectonic region, time-dependent catalog incompleteness, and inter-sequence variability, *Bull. Seismol. Soc. Am.* **106,** no. 5, 2290–2301.

Papadopoulos, A. N., P. Bazzurro, and W. Marzocchi (2021). Exploring probabilistic seismic risk assessment accounting for seismicity clustering and damage accumulation: Part I. Hazard analysis, *Earthq. Spectra* **37,** no. 2, 803–826.

Reasenberg, P., and L. Jones (1989). Earthquake hazard after a mainshock in California, *Science* **243,** 1173–1175.

Rietbrock, A., F. Strasser, and B. Edwards (2013). A stochastic earthquake ground-motion prediction model for the United Kingdom, *Bull. Seismol. Soc. Am.* **103,** no. 1, 57–77.

Sipcic, N., M. Kohrangi, A. N. Papadopoulos, W. Marzocchi, and P. Bazzurro (2022). The effect of seismic sequences in probabilistic seismic hazard analysis, *Bull. Seismol. Soc. Am.* doi: 10.1785/0120210208.

Tromans, I. J., G. Aldama-Bustos, J. Douglas, A. Lessi-Cheimariou, S. Hunt, M. Daví, R. M. W. Musson, G. Garrard, F. O. Strasser, and C. Robertson (2019). *Probabilistic Seismic Hazard Assessment for a New-Build Nuclear Power Plant Site in the UK*, Vol. 17, Springer, Netherlands.

Utsu, T. (1961). A statistical study on the occurrence of aftershocks, *Geophys. Mag.* **30,** 521–605.

Utsu, T. (1970). Aftershocks and earthquake statistics (I): Some parameters which characterize an aftershock sequence and their interrelations, *J. Fac. Sci. Hokkaido Univ.* **3,** 129–195.

Utsu, T., and Y. Ogata (1995). The centenary of the Omari formula for a decay law of aftershock activity, *J. Phys. Earth* **43,** no. 1, 1–33.

Villani, M., Z. Lubkowski, M. Free, R. M. W. Musson, B. Polidoro, R. McCully, A. Koskosidi, C. Oakman, T. Courtney, and M. Walsh (2020). A probabilistic seismic hazard assessment for Wylfa Newydd, a new nuclear site in the United Kingdom, *Bull. Earthq. Eng.* **18,** no. 9, 4061–4089.

Wang, S., M. J. Werner, and R. Yu (2021). How well does Poissonian probabilistic seismic hazard assessment (PSHA) approximate the simulated hazard of epidemic-type earthquake sequences? *Bull. Seismol. Soc. Am.* **112,** no. 1, 508–526.

Yeo, G. L., and C. A. Cornell (2009). A probabilistic framework for quantification of aftershock ground-motion hazard in California: Methodology and parametric study, *Earthq. Eng. Struct. Dynam.* **38,** 45–60.

Zhang, J., and M. D. Shields (2018). On the quantification and efficient propagation of imprecise probabilities resulting from small datasets, *Mech. Syst. Signal Process.* **98,** 465–483.

Zhang, L., K. Goda, M. J. Werner, and S. Tesfamariam (2021). Spatiotemporal seismic hazard and risk assessment of M9.0 megathrust earthquake sequences of wood-frame houses in Victoria, British Columbia, Canada, *Earthq. Eng. Struct. Dynam.* **50,** no. 1, 6–25.

Zhang, L., M. J. Werner, and K. Goda (2018). Spatiotemporal seismic hazard and risk assessment of aftershocks of M 9 megathrust earthquakes, *Bull. Seismol. Soc. Am.* **108,** no. 6, 3313–3335.

Zhuang, J., Y. Ogata, and D. Vere-Jones (2002). Stochastic declustering of space-time earthquake occurrences, *J. Am. Stat. Assoc.* **97,** no. 458, 369–380.

Manuscript received 21 July 2021
Published online 10 May 2022